Neuropsychologia 195 (2024) 108786

Contents lists available at ScienceDirect

Neuropsychologia

journal homepage: www.elsevier.com/locate/neuropsychologia

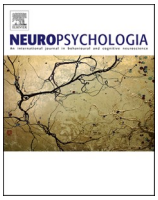

Ventral temporal and posteromedial sulcal morphology in autism spectrum disorder

Javier Ramos Benitez [a,1], Sandhya Kannan [b,1], William L. Hastings [c], Benjamin J. Parker [d], Ethan H. Willbrand [e], Kevin S. Weiner [c,d,*]

[a] Neuroscience Graduate Program, University of Washington School of Medicine, Seattle, WA, USA
[b] Department of Radiology, University of California San Francisco, San Francisco, CA, USA
[c] Department of Psychology, University of California, Berkeley, Berkeley, CA, USA
[d] Helen Wills Neuroscience Institute, University of California Berkeley, Berkeley, CA, USA
[e] Medical Scientist Training Program, School of Medicine and Public Health, University of Wisconsin–Madison, Madison, WI, USA

ARTICLE INFO

Keywords:
Autism spectrum disorder
Neuroanatomy
Brain imaging
Cortical folding
Posteromedial cortex
Ventral temporal cortex

ABSTRACT

Two parallel research tracks link the morphology of small and shallow indentations, or sulci, of the cerebral cortex with functional features of the cortex and human cognition, respectively. The first track identified a relationship between the mid-fusiform sulcus (MFS) in ventral temporal cortex (VTC) and cognition in individuals with Autism Spectrum Disorder (ASD). The second track identified a new sulcus, the inframarginal sulcus (IFRMS), that serves as a tripartite landmark within the posteromedial cortex (PMC). As VTC and PMC are structurally and functionally different in ASD, here, we integrated these two tracks and tested if there are morphological differences in VTC and PMC sulci in a sample of young (5–17 years old) male participants (50 participants with ASD and 50 neurotypical controls). Our approach replicates and extends recent findings in four ways. First, regarding replication, the standard deviation (STD) of MFS cortical thickness (CT) was increased in ASD. Second, MFS length was shorter in ASD. Third, the CT STD effect extended to other VTC and to PMC sulci. Fourth, additional morphological features of VTC sulci (depth, surface area, gray matter volume) and PMC sulci (mean CT) were decreased in ASD, including putative tertiary sulci, which emerge last in gestation and continue to develop after birth. To our knowledge, this study is the most extensive comparison of the sulcal landscape (including putative tertiary sulci) in multiple cortical expanses between individuals with ASD and NTs based on manually defined sulci at the level of individual hemispheres, providing novel targets for future studies of neurodevelopmental disorders more broadly.

1. Introduction

Understanding neuroanatomical features contributing to neurodevelopmental disorders is a major goal in cognitive and clinical neuroscience. Previous studies have identified general cortical morphological differences between individuals with Autism Spectrum Disorder (ASD) and neurotypical controls (NTs), such as cortical thickness (Bethlehem et al., 2020; Hardan et al., 2006; Khundrakpam et al., 2017; Nunes et al., 2020; Smith et al., 2016; Yang et al., 2016; Zielinski et al., 2014) and gray matter volume (Guo et al., 2021; Hazlett et al., 2006; Prigge et al., 2021; Sato et al., 2017; Seng et al., 2022; Yamasaki et al., 2010), and the morphology of the cortical folds (or sulci; Ammons et al., 2021; Auzias et al., 2014; Ecker et al., 2010; Gharehgazlou et al., 2021; Libero et al., 2019; Nordahl et al., 2007). However, the majority of these studies focused primarily on larger, earlier-developing, and more evolutionarily-conserved sulci (i.e., primary), whereas very few studies have considered the smaller, more variable, and later-developing sulci (i.e., putative tertiary sulci; Armstrong et al., 1995; Chi et al., 1977; Miller et al., 2021a, 2021b; Petrides, 2019; Sanides, 1964; Weiner, 2019; Willbrand et al., 2023; Welker, 1990). Tertiary sulci, which are located in association cortices, are also typically the smallest and shallowest cortical indentations morphologically (Amiez et al., 2018, 2019, 2021; Armstrong et al., 1995; Chi et al., 1977; Hathaway et al., 2023; Lopez-Persem et al., 2019; Maboudian et al., 2023; Miller et al., 2020,

* Corresponding author. Department of Psychology, University of California, Berkeley, Berkeley, CA, USA.
E-mail address: kweiner@berkeley.edu (K.S. Weiner).
[1] Equal contribution.

https://doi.org/10.1016/j.neuropsychologia.2024.108786
Received 5 June 2023; Received in revised form 14 December 2023; Accepted 2 January 2024
Available online 3 January 2024
0028-3932/© 2024 Published by Elsevier Ltd.

2021b; Sanides, 1964; Voorhies et al., 2021; Weiner, 2019; Weiner et al., 2014, 2018; Welker, 1990; Willbrand et al., 2022a, 2022b, 2023a, 2023b, 2023c, 2023d; Yao et al., 2022). Here, we use the term "putative tertiary sulci" to refer to sulci in VTC and PMC that are small and shallow in each cortical expanse. Nevertheless, classification of sulci as "tertiary" is classically based on gestational emergence (Armstrong et al., 1995; Chi et al., 1977; Garcia et al., 2018; Sanides, 1964; Welker, 1990) and these studies did not consider the newly classified small, shallow, and variable sulci in PMC and VTC discussed here, which can be determined in future studies leveraging freely available fetal neuroimaging datasets.

Most relevant to the present study, two recent studies have implicated the role of the latter sulci in neurodevelopmental disorders in two ways. First, the shallow mid-fusiform sulcus (MFS) in ventral temporal cortex (VTC) was shorter in individuals with developmental prosopagnosia (DP) compared to neurotypical controls (NTs), and individual differences in MFS length also related to individual differences in face perception ability (Parker et al., 2023). Second, the cortical thickness of the MFS in ASD individuals was recently shown to be more variable and negatively correlated with a behavioral task that tests an individual's ability to interpret mental states and emotions from facial features in ASD individuals (Ammons et al., 2021). Given these previous findings, the present study aimed to replicate and extend these findings by comparing the morphology of VTC sulci between ASD and NT participants (as in Ammons et al., 2021) by also considering additional VTC sulci and morphological features not previously studied.

In addition to VTC, previous work shows that the posteromedial cortex (PMC) is structurally and functionally different in individuals with ASD compared to NTs (Haghighat et al., 2021; Leech and Sharp, 2014; Lynch et al., 2013; Oblak et al., 2010, 2011). Additionally, previous studies found cytoarchitectural differences in the PMC of individuals with ASD compared to NTs (Oblak et al., 2011), as well as decreased binding sites for GABAergic receptors in the superficial and deep layers of PMC in ASD individuals compared to NTs (Oblak et al., 2010). Crucially, recent work has clarified the sulcal organization of PMC and uncovered the presence of a novel, consistent putative tertiary sulcus, the inframarginal sulcus (ifrms), that is related to the functional and anatomical organization of PMC (Willbrand et al., 2022a). Accordingly, these PMC sulci have yet to be characterized in ASD individuals. To fill this gap in knowledge, we compared the morphological features of PMC sulci between ASD and NT participants.

Together, the goals of the present study were threefold: i) attempt to replicate previous work (Ammons et al., 2021) and to quantitatively compare VTC sulcal morphology between individuals with ASD and NTs, ii) to extend these analyses to other VTC sulci and morphological features not previously studied, and iii) to assess whether these morphological similarities and differences extend to PMC sulci. To our knowledge, this study is the most extensive comparison of the sulcal landscape (including putative tertiary sulci) in multiple cortical expanses between individuals with ASD and NTs based on manually defined sulci at the level of individual hemispheres (2563 sulci in 200 hemispheres).

2. Materials and Methods

This study utilized data from the Autism Brain Imaging Data Exchange (ABIDE; Di Martino et al., 2014). Below, we detail each aspect of this multimodal dataset used for the present study.

2.1. Participants

We leveraged data from the ABIDE dataset (http://fcon_1000.projects.nitrc.org/indi/abide/abide_II.html), as it is an open-source neuroimaging database. Given limitations of this dataset resulting from 1) females being historically underdiagnosed for ASD and less present in the ABIDE sample (ASD; for examples see (Fombonne, 2009; Halladay et al., 2015; Loomes et al., 2017), as well as 2) the large developmental age range of the ABIDE samples (from childhood through young adulthood), we specifically selected participants that were 1) male and 2) less than 20 years old. We also checked whether participants' scans contained errors or artifacts (given the issues with scan quality for participants with ASD; Nordahl et al., 2016). In total, we randomly selected 100 participants in total fitting these criteria (50 participants in each group). In sum, this sample consisted of 69 participants from the New York University sample (age range 5–17 years, 41 participants with ASD, 28 NTs), 25 from the Georgetown University sample (age range 8–13 years, 5 participants with ASD, 20 NTs), and 6 from the Stanford University sample (age range 10–12 years, 4 participants with ASD, 2 NTs) that met these criteria. The ages of participants with ASD and NTs were comparable (Supplemental Table 1). See Supplemental Table 1 for additional demographic details for this sample. We chose to exclude IQ in our analyses (values presented in Supplemental Table 1) due to its (i) lack of specificity as a cognitive and neuroanatomical measure (Dennis et al., 2009; Slocombe, 1926, 1927), (ii) lack of predictive validity in group differences between NTs and ASD individuals (Dennis et al., 2009), and (iii) the cultural and socioeconomic biases that further obfuscate its place in neurodevelopmental disorders research (e.g., Turkheimer et al., 2003).

2.2. Neuroanatomical data

Imaging acquisition: All participants who participated in the study completed a mock scanning session in order to become acclimated to the scanning environment. Standard T1-weighted MPRAGE anatomical scans (TR = 2530 ms, TE = 3.25 ms, 1.3 × 1 × 1.3 mm^3 voxels) were acquired for cortical morphometric analyses in these participants using a 3 T Siemens Allegra MRI scanner at New York University Langone Medical Center, the Center for Functional and Molecular Imaging at Georgetown University, and Stanford School of Medicine Richard M. Lucas Service Center for Imaging.

Cortical surface reconstruction: Cortical surface reconstructions were generated for each participant from their T1-weighted image (downloaded from the ABIDE database) using a standard FreeSurfer pipeline (Dale et al., 1999; Fischl et al., 1999a, 1999b); FreeSurfer (v6.0): surfer.nmr.mgh.harvard.edu/). Again, we leveraged strict inclusion criteria such that we did not use any participant whose cortical surface reconstructions presented any artifacts or errors. The manual identification of sulci and the anatomical metrics extracted from those labels were calculated on each cortical surface in each participant's native space.

2.3. Regions of interest (ROIs) and sulcal labeling procedure

Ventral Temporal Cortex: As in our previous work across ages (Weiner et al., 2014), species (Miller et al., 2020), and individuals with Developmental Prosopagnosia (2% of the population who cannot perceive faces, but do not have brain damage; Parker et al., 2023), three sulci were manually identified in the VTC for each hemisphere: the Collateral Sulcus (CoS), Occipito-Temporal Sulcus (OTS), and Mid-Fusiform Sulcus (MFS). A three-tiered approach was implemented to manually label each of these three sulci in every hemisphere. First, the FG was identified as the major gyrus in VTC. Second, once the FG was identified, the OTS, CoS, and MFS were identified based on the following criteria: 1) the CoS was identified as a deep and long sulcus identifying the medial extent of the FG, 2) the OTS was identified as a deep and long sulcus identifying the lateral extent of the FG, and 3) the MFS was identified as either a single shallow longitudinal sulcus dividing the FG into lateral and medial partitions or it was identified as two or more shallow sulcal components dividing the FG into lateral and medial partitions. Third, as the MFS has predictable anterior (posterior extent of the hippocampus) and posterior (posterior transverse collateral sulcus) landmarks, but the OTS and CoS can extend longitudinally from the occipital pole to the temporal pole, we restricted our OTS and CoS definitions to the portions in VTC surrounding the MFS. This is consistent with our previous

protocols and assures that the portions of the OTS and CoS being compared to the MFS are within the VTC and are approximately equal along the length of the three sulci. Further, this restriction assures that any morphological differences between groups are not due to the fact that the OTS and CoS are much longer than the MFS, for example. Example hemispheres are shown in Fig. 1 (Supplementary Figs. 1 and 2 for all participants).

Posteromedial Cortex (PMC): Within the PMC, we identify sulci based on the recent proposal by Petrides (2019) and recent work in individual participants that builds on this work (Willbrand et al., 2023a,c). The PMC consists of the precuneus (PrC), posterior cingulate cortex (PCC), and retrosplenial cortex (RSC; Foster and Parvizi, 2017; Parvizi et al., 2006; Willbrand et al., 2022a). Based on prior work (Willbrand et al., 2022a), the PrC can be defined by the following anterior, posterior, and inferior boundaries in the medial parietal cortex: the marginal ramus of the cingulate sulcus (MCGS), the parieto-occipital sulcus (POS), and splenial sulcus (SPLS), respectively. Conversely, the PCC is bounded by the cingulate sulcus (CGS), MCGS, and SPLS superiorly, callosal sulcus (CAS) inferiorly, and POS posteriorly.

Within the PRC, we labeled the precuneual limiting sulcus (PRCULS, which extends from the superior portion of the POS), the precuneal sulci (PRCUS), and the medial extent of the superior parietal sulcus (SPS). Specifically, while previous studies identify one to three PRCUS (Margulies et al., 2009; Ono et al., 1990; Petrides, 2019; Vogt et al., 1995, 2006), we recently identified three precuneal sulci in every hemisphere (Willbrand et al., 2022a). The PRCUS were labeled based on their position within the PrC: posterior precuneal (PRCUS-p), intermediate precuneal (PRCUS-i), and anterior precuneal (PRCUS-a) sulci. As in prior work (Willbrand et al., 2022a), we also identified the SPS when it was present entering the PrC. Within the PCC, we also defined three tertiary sulci that were recently identified. First, the inframarginal sulcus (IFRMS) is a newly identified sulcus shown to be a tripartite landmark in the human brain (Willbrand et al., 2022a). The IFRMS is typically present in every hemisphere inferior to the MCGS and anterior to the SPLS. In addition, we identify two other tertiary sulci (which are more variable across hemispheres and not identifiable in every single hemisphere): the subsplenial sulcus (SSPLS) which is inferior to the SPLS, and the posterior intracingulate sulcus (ICGS-p) which is anterior to the IFRMS. Example hemispheres are shown in Fig. 2 (Supplementary Figs. 3 and 4 for all participants).

Manual sulcal labeling: Sulci were manually defined for each individual hemisphere, blind to each group, with tksurfer tools on the FreeSurfer inflated view as described in previous publications (Miller et al., 2020, 2021b; Voorhies et al., 2021; Willbrand et al., 2022a, 2023c). *Pial*, *inflated*, and *smooth* surfaces were used to determine the boundaries between intersecting sulci. Sulcal labels were defined in a three-step procedure as in our previous work (Miller et al., 2020; Parker et al., 2023; Willbrand et al., 2022a, 2023c). First, sulcal labels were defined manually by trained raters (J.R., S.K., and W.H.). Second, trained experts (B.J.P. and E.H.W.) checked these labels. Third, these labels were checked and finalized by a neuroanatomist (K.S.W.). The label definition process was completed in a blind fashion in all hemispheres before conducting morphological analyses of sulcal labels within and between groups.

Calculating the amount of cortex buried in VTC and PMC across groups: To quantitatively test whether the number of sulci in VTC and PMC was a driving factor in the regional differences in the effects observed in the **Results**, we sought to compare the amount of cortex buried in sulci between VTC and PMC. That is, even though there are more sulci in PMC than VTC, the amount of cortex within sulci could be preserved between the two cortical expanses. To test this, we combined six regions in the Destrieux parcellation (Destrieux et al., 2010) corresponding to PMC (*G_cingul-Post-dorsal, G_cingul-Post-ventral, G_precuneus, S_cingul-Marginalis, S_parieto_occipital, and S_subparietal*) and the three corresponding to VTC (*S_oc-temp_med-Lingual, G_oc-temp_lat-fusifor, and S_oc-temp_lat;* https://surfer.nmr.mgh.harvard.edu/fswiki/CorticalParcellation). These labels were converted from the Destrieux annotation into individual labels and combined into one "PMC ROI" and "VTC ROI" FreeSurfer label with the *mri_annot2label* and *mri_mergelabels* functions in FreeSurfer. To quantify the areas of the cortex defined as sulci, we used the. curv file—the file used to discriminate sulci from gyri in FreeSurfer surfaces (https://surfer.nmr.mgh.harvard.edu/) and in our prior work (e.g., Miller et al., 2021b, 2020; Parker et al., 2023; Voorhies et al., 2021; Willbrand et al., 2023c, 2022a). To create a "sulci ROI" FreeSurfer

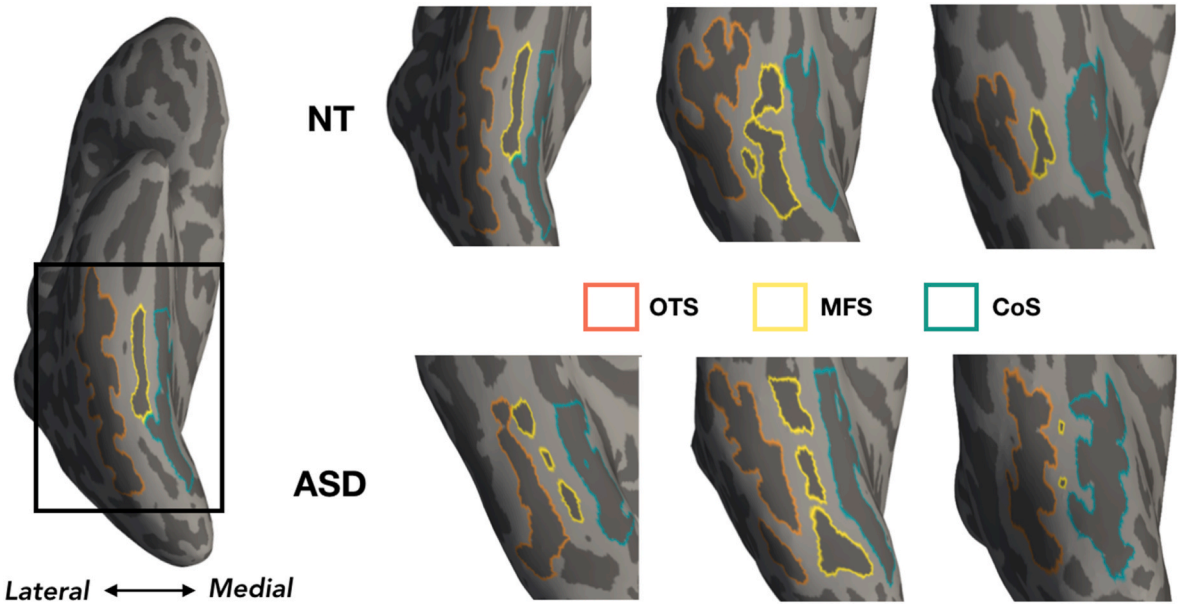

Fig. 1. Sulci of interest in ventral temporal cortex (VTC). *Left:* One example of an inflated cortical surface indicating the location (rectangle) of the zoomed portions indicated on the right. *Right:* Three example inflated cortical surface reconstructions of right hemispheres from NTs (top) and individuals with ASD (bottom). The leftmost hemisphere displays the mid-fusiform sulcus (MFS) at mean length, the center at max length, and the rightmost at minimum length in each respective group. The MFS is outlined in yellow, as well the portions of the collateral sulcus (CoS) in teal and the occipito-temporal sulcus (OTS) in red in VTC. Dark gray: sulci. Light gray: gyri.

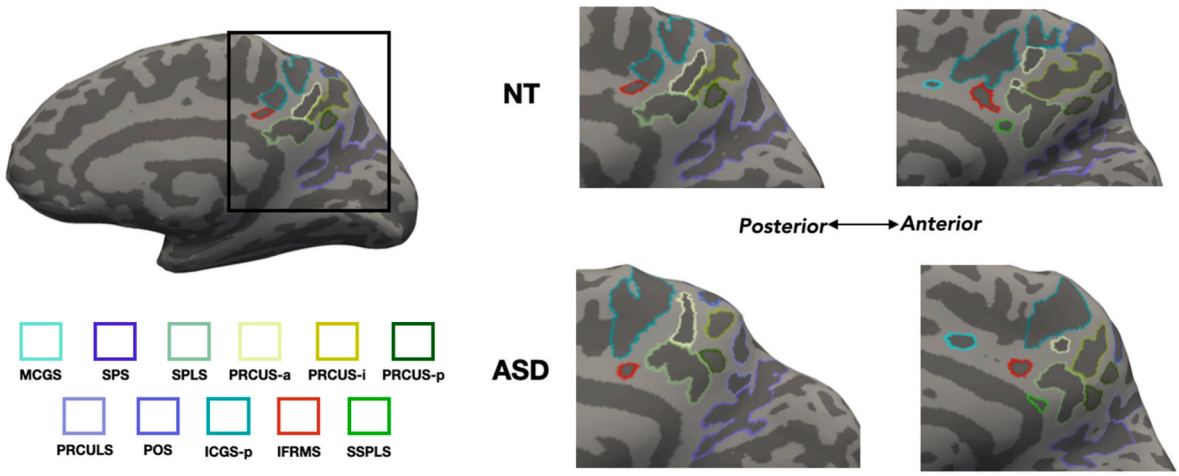

Fig. 2. Sulci of interest in posteromedial cortex (PMC). *Left:* One example of an inflated cortical surface indicating the location (rectangle) of the zoomed portions indicated on the right. *Right:* Two example inflated cortical surface reconstructions of right hemispheres from NTs (top) and individuals with ASD (bottom). The leftmost images display right hemispheres with only the ifrms present, and the rightmost images display the variable tertiary sulci present in the PMC in both groups (sspls, green; icgs-p, teal).

label, we thresholded the. curv file for all vertices with values > 0 with the *mri_binarize* function in FreeSurfer (i.e., vertices denoted as sulci). To determine the percent of PMC composed of sulci, we calculated the overlap between the PMC and VTC ROIs and sulci ROI with the Dice coefficient (Miller et al., 2021b; Willbrand et al., 2022a, 2023c).

$$DICE\ (X, Y) = \frac{2\,|X \cap Y|}{|X| + |Y|}$$

2.4. Morphological analyses

Extraction of morphological features: Considering that shallow depth and smaller surface area (SA) are defining characteristic features of putative tertiary sulci compared to primary and secondary sulci, our main focus was on mean sulcal depth and total SA. We also calculated the max sulcal depth (known as the sulcal pit), which is considered the first point of a sulcus to pull in development and is considered to be particularly relevant in the development of functional regions in gyrencephalic brains (Natu et al., 2021; Rakic, 1988; Régis et al., 2005). Additionally, we also considered mean cortical thickness (CT; mm) and total gray matter volume (GMV; mm^3), which are common morphological features explored in previous neuroimaging studies. Finally, we also quantified the standard deviation of cortical thickness (CT STD; mm) in each group as a recent study showed that the CT STD of the MFS was greater in ASDs compared to NTs (Ammons et al., 2021) with a comparable sample size. Mean and max sulcal depth values (in standard FreeSurfer units) were computed in native space from the. sulc file generated in FreeSurfer (Dale et al., 1999; Fischl et al., 1999a, 1999b). Briefly, depth values are calculated based on how far removed a vertex is from what is referred to as a "mid-surface," which is determined computationally so that the mean of the displacements around this "mid-surface" is zero. Thus, generally, gyri have negative values, while sulci have positive values. Given the shallowness and variability in the depth of tertiary sulci (Miller et al., 2020, 2021b; Parker et al., 2023; Voorhies et al., 2021; Willbrand et al., 2023a,a,c,d; Yao et al., 2022)(), some mean depth values extend below zero. We emphasize that this just reflects the metric implemented in FreeSurfer. All other morphological characteristics were calculated using the *mris_anatomical_stats* function (Fischl and Dale, 2000).

Given recent findings showing that a) the MFS is shorter in individuals with developmental prosopagnosia compared to NTs and b) MFS length is correlated with face perception ability (Parker et al., 2023), we also calculated MFS length (mm) for each participant. As in our previous work (Miller et al., 2020; Parker et al., 2023), we calculated length as the longest geodesic distance along the cortical surface between any pair of vertices on the border of the MFS label. When sulci were identified as consisting of multiple disconnected pieces on the cortical surface, the sulcal length was defined as the total length of each sulcal component [excluding the annectant gyral component(s)]. Here, the geodesic distance was calculated on the fiducial surface using algorithms implemented in the Pycortex software package (https://gallantlab.github.io/).

Morphological comparisons between ASD and NT participants: All statistical analyses were performed using R (v4.0.4) and RStudio (v1.4). We used linear mixed-effects models (LMEs) to investigate differences between groups while also controlling for age (see Supplemental Table 1 for age range). F-tests were subsequently applied to each model [Type III Analysis of Variance (ANOVA) with Satterthwaite's method]. LMEs and ANOVA were implemented using the *lme* and *anova* functions from the *nlme* R package and the built-in R *stats* package. ANOVA effect sizes are reported as partial eta-squared (η^2), acquired with the *eta_squared* function from the *effectsize* R package. Post hoc pairwise comparisons were conducted for the significant ANOVA effects and implemented with the *emmeans* function from the *emmeans* R package. In all analyses, $p < .05$ was considered significant after controlling for multiple comparisons with the false discovery rate (FDR) method.

Considering that we selected participants from multiple sites, prior to running any tests we assessed whether site (New York University, Georgetown University, Stanford University) related to differences in sulcal morphology using LMEs with site as predictor for each group separately. The only features to show a significant difference in site was CT STD in NTs ($F(2, 58) = 11$, $p = .0014$, $\eta^2 = 0.27$) and MFS length in participants with ASD ($F(2, 55) = 6.56$, $p = .02$, $\eta^2 = 0.19$). Accordingly, we controlled for site in subsequent comparisons with these features.

We first investigated whether VTC sulcal morphology differed between groups using LMEs with predictors group (ASD, NT), VTC sulci (MFS, CoS, OTS), and hemisphere (left, right), as well as their interactions, for sulcal depth (mean, max), GMV, SA, and CT (mean, STD). Age (in all analyses), and site (when relevant) were included as covariates. Age was included due to the large, developmental age ranges (Supplemental Table 1). Group, sulcus, hemisphere, and site were considered fixed effects. Sulcus was nested within the hemisphere which was nested within subject. This analysis was primarily run to replicate and extend findings from Ammons and colleagues (Ammons et al., 2021). Additionally, to further extend this recent work (Ammons et al., 2021), we investigated group differences in MFS length using a LME [controlling for age, and site] with group and hemisphere as predictors,

as well as their interaction, for length. Once again, sulcus, hemisphere, and age were considered fixed effects and hemisphere was nested within subject. We also tested for differences in PMC sulcal morphology between groups using the same exact models, except with PMC sulci (11 PMC sulci) as a predictor instead of VTC sulci. As in prior work (Hathaway et al., 2023; Miller et al., 2020; Voorhies et al., 2021; Willbrand et al., 2022a, 2023a, 2023b, 2023c; Yao et al., 2022), cortical thickness and sulcal depth analyses also controlled for the thickest and deepest points in each hemisphere.

To test whether the amount of cortex buried within each region differed, we ran a LME with group (ASD, NT), region (PMC, VTC), and hemisphere (left, right) as predictors (controlling for age and site) for percent overlap (DICE coefficient).

3. Results

3.1. Multiple morphological features of VTC sulci differ in individuals with ASD compared to NTs

As in prior studies (Miller et al., 2020; Parker et al., 2023; Weiner

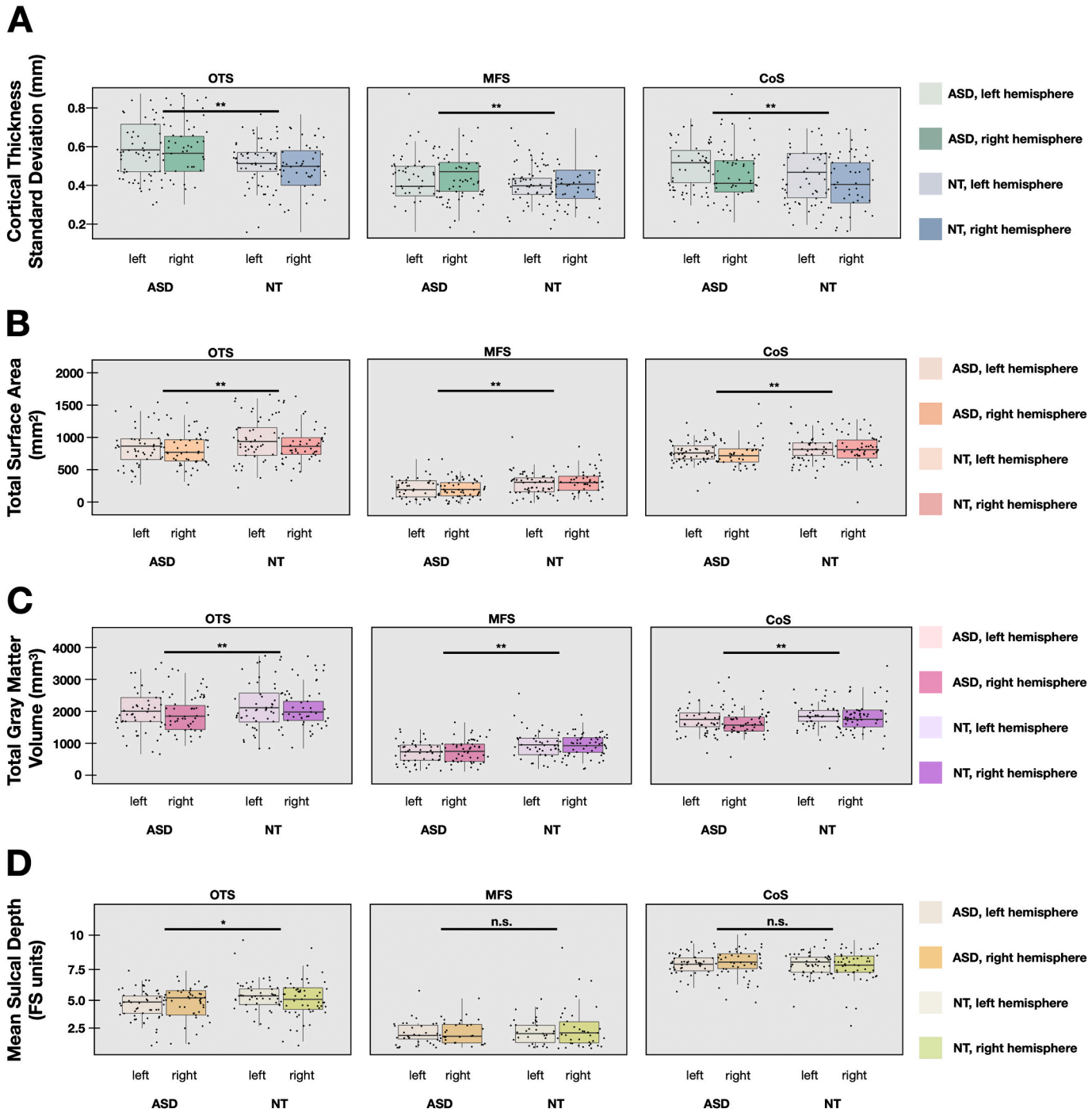

Fig. 3. Morphology of VTC sulci differs in individuals with ASD compared to NTs. A. Boxplots indicating the standard deviation (±quartile) of sulcal cortical thickness in each group (ASD; NT) for the OTS (left), MFS (middle), and CoS (right). *Left:* ASD. *Right:* NT. Lines indicate main effect of group. **B.** Same as A, but for total surface area. Lines indicate main effect of group. **C.** Same as A, but for total gray matter volume. Lines indicate the main effect of group. **D.** Same as A, but for sulcal depth. Lines indicate effects from post hoc pairwise comparisons on the group × sulcus interaction. (n.s. $p > .05$, *$p < .05$, **$p < .01$).

et al., 2014), we could identify the MFS, CoS, and OTS in all participants in both hemispheres in both groups (Fig. 1; Supplemental Table 2; see Supplementary Figs. 1 and 2 for all 600 VTC sulci across 100 participants). For each morphological feature of interest [cortical thickness (CT; mean, STD), surface area (SA), gray matter volume (GMV), and sulcal depth (mean, max)], we ran an LME with group (ASD, NT), sulcus (MFS, OTS, CoS), and hemisphere (left, right) as predictors.

We observed five effects related to group on VTC sulcal morphology. First, there was a main effect of group for CT STD ($F(1, 95) = 22.45$, $p = .000046$, $\eta^2 = 0.19$) such that there was greater variance in the CT of VTC sulci across hemispheres in ASD individuals compared to NTs (Fig. 3A; ASD Mean ± STD = 0.55 ± 0.10 mm; NT Mean ± STD = 0.51 ± 0.09 mm). Second, there was a main effect of group for SA ($F(1, 97) = 10.82$, $p = .0057$, $\eta^2 = 0.10$) such that the SA of VTC sulci across hemispheres was smaller in ASD individuals compared to NTs (Fig. 3B; ASD Mean ± STD = 639 ± 321 mm^2; NT Mean ± STD = 722 ± 361 mm^2). Third, there was a main effect of group for GMV ($F(1, 97) = 9.98$, $p = .0079$, $\eta^2 = 0.09$) such that the GMV of VTC sulci across hemispheres was less in ASD individuals compared to NTs (Fig. 3C; ASD Mean ± STD = 1541 ± 711 mm^3; NT Mean ± STD = 1735 ± 800 mm^3). Fourth, there was a marginal group × sulcus interaction for mean sulcal depth after correcting for multiple comparisons ($F(2, 392) = 3.22$, $p = .11$, $\eta^2 = 0.02$). Therefore, we implemented post hoc pairwise comparisons, which found that the difference for the OTS was significant (estimate = −0.42, $p = .025$, Tukey's adjustment), while the difference for the MFS was marginal (estimate = −0.29, $p = .11$, Tukey's adjustment; Fig. 3D) and the difference for the CoS was not significant ($p = .31$, Tukey's adjustment; Fig. 3D). Finally, there were no main effects of group on CT mean ($F(1, 97) = 2.13$, $p = .31$; Supplementary Fig. 5), mean sulcal depth ($F(1, 97) = 2.54$, $p = .27$; Fig. 3D), and max sulcal depth ($F(1, 97) = 2.30$, $p = .30$; Supplementary Fig. 5), or group-related interactions (*ps* > .34; Fig. 3; Supplementary Fig. 5).

3.2. The MFS is shorter in ASD individuals compared to NTs

Given recent work identifying a shorter MFS in individuals with developmental prosopagnosia compared to NTs (Parker et al., 2023), we tested whether the length of the MFS (in mm) differed between ASD and NT participants using an LME (controlling for age and site) with group (ASD, NT) and hemisphere (left, right) as predictors. There was a main effect of group ($F(1, 95) = 11.32$, $p = .0055$, $\eta^2 = 0.11$), in which individuals with ASD had a shorter MFS than NTs in both hemispheres (Fig. 4; ASD Mean ± STD = 32.42 ± 11.01 mm; NT Mean ± STD = 37.79 ± 11.47 mm). There was no hemisphere main effect or interaction (*ps* > .93).

3.3. Greater variance in the CT of PMC sulci in individuals with ASD compared to NTs

Similar to recent findings (Willbrand et al., 2022a), the three most prominent sulci in PMC—the MCGS, POS, and SPLS—were identifiable in all hemispheres and groups in our sample (Supplemental Table 2). The majority of PMC sulci were also present within all hemispheres (Supplemental Table 2). In addition, the SPS was present within PMC in the majority of hemispheres in both groups (Supplemental Table 2). Within PCC, the IFRMS was identifiable in all but one left and right hemisphere, whereas the other two PCC sulci (SSPLS and ICGS-p) were more variable (Supplemental Table 2; Supplementary Figs. 3 and 4 for all 1963 PMC sulci defined across the 100 participants). As in VTC, the same LMEs were run for each morphological feature of the PMC sulci [cortical thickness (CT; mean, STD), surface area (SA), gray matter volume (GMV), and sulcal depth (mean, max)].

We observed three group-related effects. First, there was a main effect of group for CT STD ($F(1, 95) = 12.66$, $p = .0032$, $\eta^2 = 0.12$) such that across all PMC sulci, the variance in CT was greater in individuals with ASD compared to NTs across hemispheres (Fig. 5; ASD Mean ± STD = 0.50 ± 0.13 mm; NT Mean ± STD = 0.47 ± 0.12 mm). Second, there was a significant group × sulcus interaction ($F(10, 1723) = 2.70$, $p = .014$, $\eta^2 = 0.02$). Post hoc pairwise comparisons revealed that this interaction was driven by four PMC sulci having higher CT STD in individuals with ASD compared to NTs (Fig. 5): i) SSPLS (estimate = 0.10, $p = .0001$, Tukey's adjustment), ii) ICGS-p (estimate = 0.05, $p = .027$, Tukey's adjustment), iii) MCGS (estimate = 0.04, $p = .031$, Tukey's adjustment), and iv) PRCULS (estimate = 0.04, $p = .012$, Tukey's adjustment). Third, there was a marginal group × sulcus interaction for mean CT after correcting for multiple comparisons ($F(10, 1723) = 2.16$, $p = .068$, $\eta^2 = 0.01$). Here, post hoc pairwise comparisons confirmed that only a subset of PMC sulci were either significantly or marginally thinner in participants with ASD compared to NTs (Fig. 6; all other PMC sulci in Supplementary Fig. 6): the SSPLS (estimate = −0.21, $p = .0024$, Tukey's adjustment) and ICGS-p (estimate = −0.19, $p = .0043$, Tukey's adjustment) were significantly thinner in participants with ASD compared to NTs. There were no other significant main effects of group on the other morphological features: mean sulcal depth ($F(1, 97) = 0.063$, $p = .87$; Supplementary Fig. 7), max sulcal depth ($F(1, 97) = 0.13$, $p = .85$; Supplementary Fig. 8), SA ($F(1, 97) = 0.23$, $p = .78$; Supplementary Fig. 9), GMV ($F(1, 97) = 1.04$, $p = .52$; Supplementary Fig. 10), or group-related interactions (*ps* > .13; Supplementary Figs. 6–10).

3.3.1. Comparing the amount of cortex buried in sulci in VTC and PMC

Finally, to compare how much of the VTC and PMC is sulcal vs. gyral between groups, we calculated how much of the regions corresponding to an automated parcellation of VTC and PMC in FreeSurfer (Destrieux et al., 2010) were buried in sulci (i.e., the percentage of vertices with

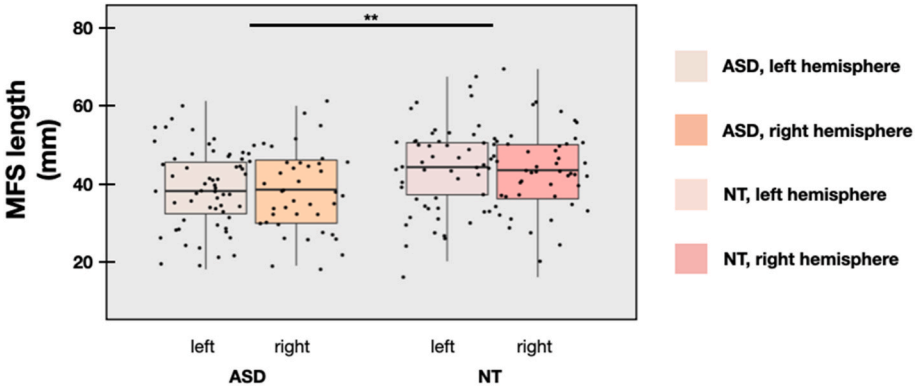

Fig. 4. The MFS is longer in NTs compared to participants with ASD. Boxplots indicating MFS length (±quartile) in each group. *Left:* ASD. *Right:* NT. Line indicates the significant main effect of group. (**p < .01).

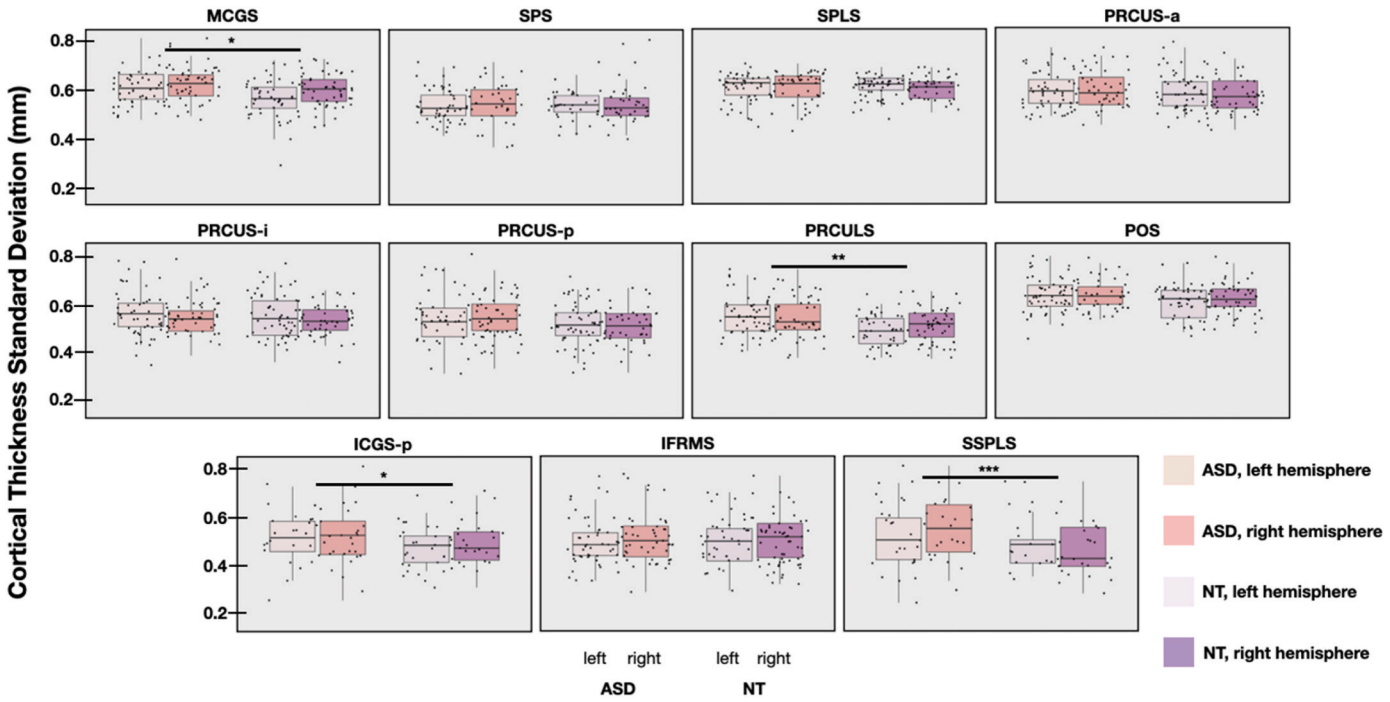

Fig. 5. The thickness of PMC sulci is more variable in individuals with ASD compared to NTs. Boxplots indicating the standard deviation (±quartile) of sulcal cortical thickness (CT STD) in each group (ASD; NT). *Left:* ASD. *Right:* NT. Lines indicate effects from post hoc pairwise comparisons on the group × sulcus interaction. (*p < .05, **p < .01, ***p < .001).

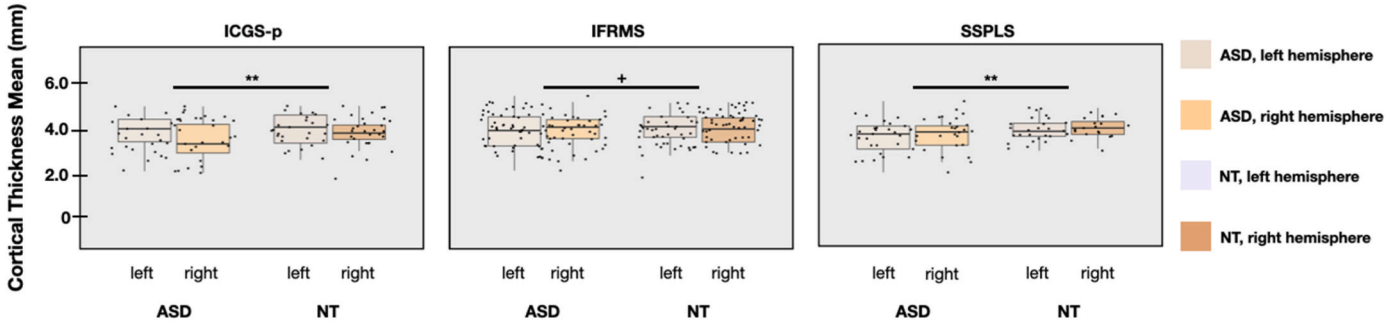

Fig. 6. Mean cortical thickness of PCC putative tertiary sulci was larger in NTs compared to participants with ASD. Boxplots indicating mean cortical thickness (CT; ± quartile) in each group (ASD; NT). *Left:* ASD. *Right:* NT. Lines indicate effects from post hoc pairwise comparisons on the group × sulcus interaction. (+ p < .10, *p < .05, **p < .01).

values above zero in the. curv file; (Dale et al., 1999) via the Dice coefficient (**Materials and Methods**). Consistent with prior work (Van Essen, 2007; Vogt et al., 1995; Willbrand et al., 2023c; Zilles et al., 1988), the majority of human VTC (Mean ± STD = 72.17 ± 1.75%) and PMC (Mean ± STD = 69.19 ± 1.17%) was buried in sulci. Comparing the overlap with an LME with group (ASD, NT), region (PMC, VTC), and hemisphere (left, right) as predictors (controlling for age and imaging site) revealed no group-related effects on the amount of sulci in PMC or VTC (*ps* > .64). Therefore, the presence of group differences in more morphological features in VTC than PMC at the individual sulcal-level is not due to group differences in the amount of sulci in each region—further emphasizing the importance of assessing differences at the level of individual sulci.

4. Discussion

To our knowledge, this study is the most extensive comparison of the sulcal landscape (including putative tertiary sulci) in multiple cortical expanses between individuals with ASD and NTs based on manually defined sulci at the level of individual hemispheres, providing novel targets for future studies of neurodevelopmental disorders more broadly (Ammons et al., 2021). Our analyses revealed morphological differences of VTC and PMC sulci between groups with five main findings. First and second, the largest effect was that individual differences in cortical thickness across VTC and PMC sulci were larger in individuals with ASD compared to NTs—replicating and extending previous findings (Ammons et al., 2021) to other sulci in VTC aside from the MFS, as well as to PMC sulci. Third, additional sulcal metrics (surface area, gray matter volume, and mean sulcal depth) were decreased in VTC sulci in participants with ASD compared to NTs. Fourth, the MFS was shorter in individuals with ASD compared to NTs, which is consistent with recent findings showing that the MFS is also shorter in individuals with developmental prosopagnosia compared to NTs (Parker et al., 2023). Fifth, the gray matter thickness of the most variable putative tertiary sulci in PCC (Willbrand et al., 2022a) was decreased in participants with ASD compared to NTs. Below, we discuss these findings in the context of i) the morphology of the mid-fusiform sulcus in neurodevelopmental disorders, ii) underlying white matter architecture contributing to the

relationships identified here such as potential white matter tracts connecting sulci in VTC and PMC, and iii) the limitations and future directions of the present study.

4.1. On the morphology of the mid-fusiform sulcus and other putative tertiary sulci in neurodevelopmental disorders

Our findings build on a growing number of studies documenting the role of the MFS in neurodevelopmental disorders (Ammons et al., 2021; Hettwer et al., 2022; Parker et al., 2023). For example, in VTC, three recent studies found a relationship between anatomical features of either the FG at the location of the MFS or the MFS morphology in particular, in different neurodevelopmental disorders. Specifically, Ammons and colleagues (Ammons et al., 2021) found morphological differences in the MFS of ASD participants when compared to NTs. In particular, MFS cortical thickness was more variable in participants with ASD and significantly correlated with the ability to interpret emotion and infer mental states from facial features. Additionally, recent work examining morphological features of the MFS in developmental prosopagnosia revealed that the MFS was significantly shorter in developmental prosopagnosics compared to NTs and that MFS length also predicted face perception ability (Parker et al., 2023). Finally, recent work (Hettwer et al., 2022) identified that the morphology of the right FG was positively correlated with schizophrenia polygenic resilience scores overlapping with the location of the MFS at the group level. Thus, the combination of these and our present findings indicates that MFS length is likely a transdiagnostic factor, and that future work performing morphological analyses at the level of individual participants in additional populations may further empirically support, as well as clarify, the role of MFS morphology in a growing number of neurodevelopmental disorders. Considering that the MFS is a microarchitectonic and functional landmark (Weiner, 2019), alterations in MFS length could be a marker for alterations in these features—a testable hypothesis that can be addressed in future multimodal investigations in neurotypical and clinical populations.

Beyond VTC, the present findings also incorporate novel PMC sulci for the first time and show that, like VTC (Ammons et al., 2021), individual differences in the variability of PMC sulcal thickness is greater in individuals with ASD compared to NTs. Therefore, this relationship between ASD and the variability of sulcal morphology in association cortices appears to be a replicable effect across cortical expanses. Future work should seek to determine whether this relationship extends to the many sulci within other regions, such as prefrontal cortex (Garrison et al., 2015; Hardan et al., 2004; Nakamura et al., 2020; Voorhies et al., 2021; Willbrand et al., 2022b), which contains several small, shallow, and variable sulci. In addition, the mean thickness of the most variable PMC sulci was particularly decreased in participants with ASD, which motivates future studies to understand what anatomical and functional features are affected by the presence/absence of these PMC sulci in a given hemisphere not only in individuals with ASD, but also other neurodevelopmental disorders, as well as other neurological and psychiatric disorders (such as Alzheimer's disease and schizophrenia;Leech and Sharp, 2014). Such analyses would also determine whether effects to the gray matter of these PMC sulci are transdiagnostic or unique to ASD.

4.2. White matter tracts connecting consistent and variable VTC and PMC sulci?

Considering the differences in sulcal morphology observed in both PMC and VTC, as well as theories linking sulcal morphology to underlying white matter (Van Essen, 1997, 2020; Welker, 1990), we hypothesize that presently unidentified corticocortical projections between sulci within VTC and PMC may be different in ASD participants compared to NTs.

These ideas are in line with recent studies showing that a vertical component of the cingulum bundle connects PMC with VTC. For instance, Jones and colleagues (Jones et al., 2013) found that a minority of cingulum bundle fibers were divided into three sections based on the trajectory of their fibers, one of which connects the cingulate with ventral temporal regions. Jones et al. (2013) referred to this bundle as the "restricted parahippocampal cingulum", and recognized that further examination was required to better understand its functional value as well as to better characterize the specific projections of the bundle. Additionally, Wu and colleagues (Wu et al., 2016) dissected the cingulum bundle into five segments, one of which they referred to as Cingulum Bundle V (CB–V), which also connected the PMC to VTC. Similar observations were also made by Skandalakis and colleagues (Skandalakis et al., 2020), who noted that the functional role, as well as clinical implications of this bundle, were presently lacking. Thus, future studies can test the following hypotheses, if: i) CB-V connects the PMC sulci to the MFS and ii) features of CB-V are different in ASD and NT participants.

In terms of the former, recent research identifies a "medial face area" in PMC (Silson et al., 2019; Woolnough et al., 2020), which begs the question if there is a relationship between (i) sulcal morphology and this face-selective region, (ii) the endpoints of CB-V and the location of this PMC face-selective region, and (iii) PMC sulcal morphology and face processing ability. In direct relation to VTC and PMC, Silson et al. (2019) showed that regions lateral to the MFS are functionally connected (as measured by resting state fMRI) to PMC regions. Thus, future studies could incorporate functional neuroimaging data related to face processing and functional connectivity, as well as behavioral measures of face processing ability, to test if sulcal morphology plays a role in this complex relationship among anatomy, functional representations in VTC and PMC, and face perception—and further, compare this potential relationship between ASD individuals and NTs.

4.3. Future directions and limitations

The findings from the present study provide a foundation for future studies. First, while the present study compared sulcal morphology between ASD participants and NTs, it did not examine the relationship between sulci and functional representations. For example, the IFRMS has recently been shown to identify a node of the cognitive control network in PMC (Willbrand et al., 2022a) and face-selective regions have been recently identified in PMC (Silson et al., 2019; Woolnough et al., 2020), while the MFS identifies functional transitions in many functional maps and also, predicts the location of face-selective regions (Grill-Spector and Weiner, 2014; Weiner, 2019). Thus, future studies can also quantify the relationship of sulci to these different functional representations in ASD participants and NTs, and then compare this relationship between groups. Second, as mentioned at the end of the previous section, an analysis of integrity differences in the CB-V between ASD participants and NTs using diffusion-weighted imaging would provide insights regarding the clinical implications of this bundle. Third, although we did not observe any group × hemispheric interactions in our analyses, future studies should explore lateralization differences between ASD participants and NTs in both the anatomical, as well as the functional, organization of sulcal morphology in VTC and PMC.

We end this section by acknowledging six main limitations of the present study. First, the scope of the present study was limited to males and younger participants as older and female participants with ASD are scarce (**Materials and Methods**). Future analyses of these samples are necessary to determine whether these effects differ depending on the age and gender of the participants. Second, longitudinal analyses were not possible since subsequent scan sessions are not available. Third, work by Pua et al. (2019) demonstrated a relationship among cortical thickness, symptom severity, and cognitive performance while also highlighting the contribution of region-specific morphological variability patterns to behavioral phenotypes. While these analyses are highly informative, they lay outside the scope of the present manuscript. Future work will

aim to explore the morphological features observed in our work and their relationship with cognition and behavioral phenotype in greater detail. Fourth, recent work (Mei et al., 2023) shows that total variance in morphological features heavily contributed to the severity of ASD core symptoms quantified by the behavioral battery ADOS-2. These observations are highly informative about morphological patterns and their influence on behavioral phenotypes in ASD, making the significant undertaking of characterizing said similarities in the context of putative tertiary sulci a target for future research. Fifth, we did not analyze the relationship between VIQ, PIQ, and FIQ (Supplemental Table 1) with sulcal morphology scores as it (along with other behavioral metrics) are largely outside of the scope of this paper. Furthermore, these metrics were not analyzed in prior work on MFS morphology in ASD (Ammons et al., 2021). Finally, while the present study had a large N in terms of sulci that were manually defined, due to the arduous, time-consuming nature of these manual definitions, our sample size of participants was relatively low compared to group-level analyses (N = 100 hemispheres in each sample), and we were only able to compare two cortical expanses as opposed to performing whole-brain analyses. To begin to ameliorate this concern, we share our sulcal definitions with the publication of this paper. As such, future sulcal definitions can be added to the same individuals analyzed in the present study in order to begin to build a whole-brain understanding of the relationship of sulcal morphology as defined in each individual and the entire cerebral cortex in NTs compared to individuals with ASD.

5. Conclusion

Building on previous work showing that VTC sulcal morphology differs between ASD participants and NTs (Ammons et al., 2021), the present study not only replicated and extended this prior work but also showed that the morphology of newly-identified sulci in PMC also differs between ASD and NT participants. These findings emphasize the importance of leveraging "precision neuroimaging" approaches to further understanding neurodevelopmental disorders at a more fine-grained scale (Gratton et al., 2022; Weiner and Willbrand, 2023). Our findings are also encouraging for the study of putative tertiary sulci in ASD in other cortical expanses and neurodevelopmental disorders, which can be explored in future studies.

CRediT authorship contribution statement

Javier Ramos Benitez: Conceptualization, Data curation, Formal analysis, Investigation, Methodology, Project administration, Resources, Validation, Visualization, Writing – original draft, Writing – review & editing. **Sandhya Kannan:** Conceptualization, Data curation, Formal analysis, Investigation, Methodology, Project administration, Resources, Validation, Visualization, Writing – original draft, Writing – review & editing. **William L. Hastings:** Data curation, Project administration. **Benjamin J. Parker:** Conceptualization, Data curation, Methodology. **Ethan H. Willbrand:** Conceptualization, Data curation, Formal analysis, Investigation, Methodology, Project administration, Resources, Validation, Visualization, Writing – original draft, Writing – review & editing. **Kevin S. Weiner:** Conceptualization, Data curation, Formal analysis, Funding acquisition, Investigation, Methodology, Project administration, Resources, Software, Supervision, Validation, Visualization, Writing – original draft, Writing – review & editing.

Declaration of competing interest

The authors declare no competing financial interests.

Data availability

Data will be made available on request.

Acknowledgments

This research was supported by NSF CAREER Award 2042251 (Weiner) and NIH Medical Scientist Training Program Grant T32 GM140935 (Willbrand). Funding for original data collection and curation for the New York University sample was provided by NIH (K23MH087770; R21MH084126; R01MH081218; R01HD065282), Autism Speaks, The Stavros Niarchos Foundation, The Leon Levy Foundation, and an endowment provided by Phyllis Green and Randolph Cowen. Funding for original data collection and curation for the Georgetown University sample was provided by NIMH MH084961, Intellectual and Developmental Disabilities Research Center, and Children's National Medical Center HD040677-07. We thank Linda Wilbrecht for providing feedback on the analysis and manuscript in its initial stages.

Appendix A. Supplementary data

Supplementary data to this article can be found online at https://doi.org/10.1016/j.neuropsychologia.2024.108786.

References

Amiez, C., Wilson, C.R.E., Procyk, E., 2018. Variations of cingulate sulcal organization and link with cognitive performance. Sci. Rep. 8, 1–13.
Amiez, C., Sallet, J., Hopkins, W.D., Meguerditchian, A., Hadj-Bouziane, F., Ben Hamed, S., Wilson, C.R.E., Procyk, E., Petrides, M., 2019. Sulcal organization in the medial frontal cortex provides insights into primate brain evolution. Nat. Commun. 10, 1–14.
Amiez, C., Sallet, J., Novek, J., Hadj-Bouziane, F., Giacometti, C., Andersson, J., Hopkins, W.D., Petrides, M., 2021. Chimpanzee histology and functional brain imaging show that the paracingulate sulcus is not human-specific. Commun. Biol. 4, 54.
Ammons, C.J., Winslett, M.-E., Bice, J., Patel, P., May, K.E., Kana, R.K., 2021. The midfusiform sulcus in autism spectrum disorder: Establishing a novel anatomical landmark related to face processing. Autism Res. 14, 53–64.
Armstrong, E., Schleicher, A., Omran, H., Curtis, M., Zilles, K., 1995. The ontogeny of human gyrification. Cerebr. Cortex 5, 56–63.
Auzias, G., Viellard, M., Takerkart, S., Villeneuve, N., Poinso, F., Fonséca, D.D., Girard, N., Deruelle, C., 2014. Atypical sulcal anatomy in young children with autism spectrum disorder. Neuroimage Clin 4, 593–603.
Bethlehem, R.A.I., Seidlitz, J., Romero-Garcia, R., Trakoshis, S., Dumas, G., Lombardo, M.V., 2020. A normative modelling approach reveals age-atypical cortical thickness in a subgroup of males with autism spectrum disorder. Commun. Biol. 3, 486.
Chi, J.G., Dooling, E.C., Gilles, F.H., 1977. Gyral development of the human brain. Ann. Neurol. 1, 86–93.
Dale, A.M., Fischl, B., Sereno, M.I., 1999. Cortical surface-based analysis. I. Segmentation and surface reconstruction. Neuroimage 9, 179–194.
Dennis, M., Francis, D.J., Cirino, P.T., Schachar, R., Barnes, M.A., Fletcher, J.M., 2009. Why IQ is not a covariate in cognitive studies of neurodevelopmental disorders. J. Int. Neuropsychol. Soc. 15, 331–343.
Destrieux, C., Fischl, B., Dale, A., Halgren, E., 2010. Automatic parcellation of human cortical gyri and sulci using standard anatomical nomenclature. Neuroimage 53, 1–15.
Ecker, C., Marquand, A., Mourão-Miranda, J., Johnston, P., Daly, E.M., Brammer, M.J., Maltezos, S., Murphy, C.M., Robertson, D., Williams, S.C., Murphy, D.G.M., 2010. Describing the brain in autism in five dimensions–magnetic resonance imaging-assisted diagnosis of autism spectrum disorder using a multiparameter classification approach. J. Neurosci. 30, 10612–10623.
Van Essen, D.C., 1997. A tension-based theory of morphogenesis and compact wiring in the central nervous system. Nature 385, 313–318.
Van Essen, D.C., 2007. 4.16 - cerebral cortical folding patterns in primates: why they vary and what they signify. In: Kaas, J.H. (Ed.), Evolution of Nervous Systems. Academic Press, Oxford, pp. 267–276.
Van Essen, D.C., 2020. A 2020 view of tension-based cortical morphogenesis. Proc. Natl. Acad. Sci. U.S.A. https://doi.org/10.1073/pnas.2016830117.
Fischl, B., Dale, A.M., 2000. Measuring the thickness of the human cerebral cortex from magnetic resonance images. Proc. Natl. Acad. Sci. U.S.A. 97, 11050–11055.
Fischl, B., Sereno, M.I., Dale, A.M., 1999a. Cortical surface-based analysis. II: inflation, flattening, and a surface-based coordinate system. Neuroimage 9, 195–207.
Fischl, B., Sereno, M.I., Tootell, R.B., Dale, A.M., 1999b. High-resolution intersubject averaging and a coordinate system for the cortical surface. Hum. Brain Mapp. 8, 272–284.
Fombonne, E., 2009. Epidemiology of pervasive developmental disorders. Pediatr. Res. 65, 591–598.
Foster, B.L., Parvizi, J., 2017. Direct cortical stimulation of human posteromedial cortex. Neurology 88, 685–691.

Garcia, K.E., Kroenke, C.D., Bayly, P.V., 2018. Mechanics of cortical folding: stress, growth and stability. Philos. Trans. R. Soc. Lond. B Biol. Sci. 373 https://doi.org/10.1098/rstb.2017.0321.
Garrison, J.R., Fernyhough, C., McCarthy-Jones, S., Haggard, M., 2015. Australian schizophrenia research bank, simons, J.S. Paracingulate sulcus morphology is associated with hallucinations in the human brain. Nat. Commun. 6, 8956.
Gharehgazlou, A., Freitas, C., Ameis, S.H., Taylor, M.J., Lerch, J.P., Radua, J., Anagnostou, E., 2021. Cortical gyrification morphology in individuals with ASD and ADHD across the Lifespan: a systematic review and meta-analysis. Cerebr. Cortex 31, 2653–2669.
Gratton, C., Nelson, S.M., Gordon, E.M., 2022. Brain-behavior correlations: two paths toward reliability. Neuron 110, 1446–1449.
Grill-Spector, K., Weiner, K.S., 2014. The functional architecture of the ventral temporal cortex and its role in categorization. Nat. Rev. Neurosci. 15, 536–548.
Guo, X., Duan, X., Suckling, J., Wang, J., Kang, X., Chen, H., Biswal, B.B., Cao, J., He, C., Xiao, J., Huang, X., Wang, R., Han, S., Fan, Y.-S., Guo, J., Zhao, J., Wu, L., Chen, H., 2021. Mapping progressive gray matter alterations in early childhood autistic brain. Cerebr. Cortex 31, 1500–1510.
Haghighat, H., Mirzarezaee, M., Araabi, B.N., Khadem, A., 2021. Functional networks abnormalities in autism spectrum disorder: age-related hypo and hyper connectivity. Brain Topogr. 34, 306–322.
Halladay, A.K., Bishop, S., Constantino, J.N., Daniels, A.M., Koenig, K., Palmer, K., Messinger, D., Pelphrey, K., Sanders, S.J., Singer, A.T., Taylor, J.L., Szatmari, P., 2015. Sex and gender differences in autism spectrum disorder: summarizing evidence gaps and identifying emerging areas of priority. Mol. Autism. 6, 36.
Hardan, A.Y., Jou, R.J., Keshavan, M.S., Varma, R., Minshew, N.J., 2004. Increased frontal cortical folding in autism: a preliminary MRI study. Psychiatr. Res. 131, 263–268.
Hardan, A.Y., Muddasani, S., Vemulapalli, M., Keshavan, M.S., Minshew, N.J., 2006. An MRI study of increased cortical thickness in autism. Am. J. Psychiatr. 163, 1290–1292.
Hathaway, C.B., Voorhies, W.I., Sathishkumar, N., Mittal, C., Yao, J.K., Miller, J.A., Parker, B.J., Weiner, K.S., 2023. Defining putative tertiary sulci in lateral prefrontal cortex in chimpanzees using human predictions. Brain Struct. Funct. https://doi.org/10.1007/s00429-023-02638-7.
Hazlett, H.C., Poe, M.D., Gerig, G., Smith, R.G., Piven, J., 2006. Cortical gray and white brain tissue volume in adolescents and adults with autism. Biol. Psychiatr. 59, 1–6.
Hettwer, M.D., Lancaster, T.M., Raspor, E., Hahn, P.K., Mota, N.R., Singer, W., Reif, A., Linden, D.E.J., Bittner, R.A., 2022. Evidence from imaging resilience genetics for a protective mechanism against schizophrenia in the ventral visual pathway. Schizophr. Bull. https://doi.org/10.1093/schbul/sbab151.
Jones, D.K., Christiansen, K.F., Chapman, R.J., Aggleton, J.P., 2013. Distinct subdivisions of the cingulum bundle revealed by diffusion MRI fibre tracking: implications for neuropsychological investigations. Neuropsychologia 51, 67–78.
Khundrakpam, B.S., Lewis, J.D., Kostopoulos, P., Carbonell, F., Evans, A.C., 2017. Cortical thickness abnormalities in autism spectrum disorders through late childhood, adolescence, and adulthood: a large-scale mri study. Cerebr. Cortex 27, 1721–1731.
Leech, R., Sharp, D.J., 2014. The role of the posterior cingulate cortex in cognition and disease. Brain 137, 12–32.
Libero, L.E., Schaer, M., Li, D.D., Amaral, D.G., Nordahl, C.W., 2019. A longitudinal study of local gyrification index in young boys with autism spectrum disorder. Cerebr. Cortex 29, 2575–2587.
Loomes, R., Hull, L., Mandy, W.P.L., 2017. What is the male-to-female ratio in autism spectrum disorder? A systematic review and meta-analysis. J. Am. Acad. Child Adolesc. Psychiatry 56, 466–474.
Lopez-Persem, A., Verhagen, L., Amiez, C., Petrides, M., Sallet, J., 2019. The human ventromedial prefrontal cortex: sulcal morphology and its influence on functional organization. J. Neurosci. 39, 3627–3639.
Lynch, C.J., Uddin, L.Q., Supekar, K., Khouzam, A., Phillips, J., Menon, V., 2013. Default mode network in childhood autism: posteromedial cortex heterogeneity and relationship with social deficits. Biol. Psychiatr. 74, 212–219.
Maboudian, S.A., Willbrand, E.H., Jagust, W.J., Weiner, K.S., Alzheimer's Disease Neuroimaging Initiative, 2023. Defining Overlooked Structures Reveals New Associations between Cortex and Cognition in Aging and Alzheimer's Disease. https://doi.org/10.1101/2023.06.29.546558 bioRxiv.
Margulies, D.S., Vincent, J.L., Kelly, C., Lohmann, G., Uddin, L.Q., Biswal, B.B., Villringer, A., Xavier Castellanos, F., Milham, M.P., Petrides, M., 2009. Precuneus shares intrinsic functional architecture in humans and monkeys. Proc. Natl. Acad. Sci. U.S.A. 106, 20069–20074.
Di Martino, A., Yan, C.-G., Li, Q., Denio, E., Castellanos, F.X., Alaerts, K., Anderson, J.S., Assaf, M., Bookheimer, S.Y., Dapretto, M., Deen, B., Delmonte, S., Dinstein, I., Ertl-Wagner, B., Fair, D.A., Gallagher, L., Kennedy, D.P., Keown, C.L., Keysers, C., Lainhart, J.E., Lord, C., Luna, B., Menon, V., Minshew, N.J., Monk, C.S., Mueller, S., Müller, R.-A., Nebel, M.B., Nigg, J.T., O'Hearn, K., Pelphrey, K.A., Peltier, S.J., Rudie, J.D., Sunaert, S., Thioux, M., Tyszka, J.M., Uddin, L.Q., Verhoeven, J.S., Wenderoth, N., Wiggins, J.L., Mostofsky, S.H., Milham, M.P., 2014. The autism brain imaging data exchange: towards a large-scale evaluation of the intrinsic brain architecture in autism. Mol. Psychiatr. 19, 659–667.
Mei, T., Forde, N.J., Floris, D.L., Dell'Acqua, F., Stones, R., Ilioska, I., Durston, S., Moessnang, C., Banaschewski, T., Holt, R.J., Baron-Cohen, S., Rausch, A., Loth, E., Oakley, B., Charman, T., Ecker, C., Murphy, D.G.M., Eu-Aims Leap group, Beckmann, C.F., Llera, A., Buitelaar, J.K., 2023. Autism is associated with interindividual variations of gray and white matter morphology. Biol Psychiatry Cogn Neurosci Neuroimaging 8, 1084–1093.
Miller, J.A., Voorhies, W.I., Li, X., Raghuram, I., Palomero-Gallagher, N., Zilles, K., Sherwood, C.C., Hopkins, W.D., Weiner, K.S., 2020. Sulcal morphology of ventral temporal cortex is shared between humans and other hominoids. Sci. Rep. 10, 17132.
Miller, J.A., D'Esposito, M., Weiner, K.S., 2021a. Using tertiary sulci to map the "cognitive globe" of prefrontal cortex. J. Cognit. Neurosci. 1–18.
Miller, J.A., Voorhies, W.I., Lurie, D.J., D'Esposito, M., Weiner, K.S., 2021b. Overlooked tertiary sulci serve as a meso-scale link between microstructural and functional properties of human lateral prefrontal cortex. J. Neurosci. 41, 2229–2244.
Nakamura, M., Nestor, P.G., Shenton, M.E., 2020. Orbitofrontal sulcogyral pattern as a transdiagnostic trait marker of early neurodevelopment in the social brain. Clin. EEG Neurosci. 51, 275–284.
Natu, V.S., Arcaro, M.J., Barnett, M.A., Gomez, J., Livingstone, M., Grill-Spector, K., Weiner, K.S., 2021. Sulcal depth in the medial ventral temporal cortex predicts the location of a place-selective region in macaques, children, and adults. Cerebr. Cortex 31, 48–61.
Nordahl, C.W., Dierker, D., Mostafavi, I., Schumann, C.M., Rivera, S.M., Amaral, D.G., Van Essen, D.C., 2007. Cortical folding abnormalities in autism revealed by surface-based morphometry. J. Neurosci. 27, 11725–11735.
Nordahl, C.W., Mello, M., Shen, A.M., Shen, M.D., Vismara, L.A., Li, D., Harrington, K., Tanase, C., Goodlin-Jones, B., Rogers, S., Abbeduto, L., Amaral, D.G., 2016. Methods for acquiring MRI data in children with autism spectrum disorder and intellectual impairment without the use of sedation. J. Neurodev. Disord. 8, 20.
Nunes, A.S., Vakorin, V.A., Kozhemiako, N., Peatfield, N., Ribary, U., Doesburg, S.M., 2020. Atypical age-related changes in cortical thickness in autism spectrum disorder. Sci. Rep. 10, 11067.
Oblak, A.L., Gibbs, T.T., Blatt, G.J., 2010. Decreased GABA(B) receptors in the cingulate cortex and fusiform gyrus in autism. J. Neurochem. 114, 1414–1423.
Oblak, A.L., Rosene, D.L., Kemper, T.L., Bauman, M.L., Blatt, G.J., 2011. Altered posterior cingulate cortical cytoarchitecture, but normal density of neurons and interneurons in the posterior cingulate cortex and fusiform gyrus in autism. Autism Res. 4, 200–211.
Ono, M., Kubik, S., Abernathey, C.D., 1990. Atlas of the Cerebral Sulci. G. Thieme Verlag.
Parker, B.J., Voorhies, W.I., Jiahui, G., Miller, J.A., Willbrand, E., Hallock, T., Furl, N., Garrido, L., Duchaine, B., Weiner, K.S., 2023. Hominoid-specific sulcal variability is related to face perception ability. Brain Struct. Funct. 228, 677–685.
Parvizi, J., Van Hoesen, G.W., Buckwalter, J., Damasio, A., 2006. Neural connections of the posteromedial cortex in the macaque. Proc. Natl. Acad. Sci. U.S.A. 103, 1563–1568.
Petrides, M., 2019. Atlas of the Morphology of the Human Cerebral Cortex on the Average MNI Brain. Academic Press.
Prigge, M.B.D., Lange, N., Bigler, E.D., King, J.B., Dean 3rd, D.C., Adluru, N., Alexander, A.L., Lainhart, J.E., Zielinski, B.A., 2021. A 16-year study of longitudinal volumetric brain development in males with autism. Neuroimage 236, 118067.
Pua, E.P.K., Ball, G., Adamson, C., Bowden, S., Seal, M.L., 2019. Quantifying individual differences in brain morphometry underlying symptom severity in Autism Spectrum Disorders. Sci. Rep. 9, 9898.
Rakic, P., 1988. Specification of cerebral cortical areas. Science 241, 170–176.
Régis, J., Mangin, J.-F., Ochiai, T., Frouin, V., Riviére, D., Cachia, A., Tamura, M., Samson, Y., 2005. "Sulcal root" generic model: a hypothesis to overcome the variability of the human cortex folding patterns. Neurol. Med.-Chir. 45, 1–17.
Sanides, F., 1964. Structure and function of the human frontal lobe. Neuropsychologia 2, 209–219.
Sato, W., Kochiyama, T., Uono, S., Yoshimura, S., Kubota, Y., Sawada, R., Sakihama, M., Toichi, M., 2017. Reduced gray matter volume in the social brain network in adults with autism spectrum disorder. Front. Hum. Neurosci. 11, 395.
Seng, G.-J., Lai, M.-C., Goh, J.O.S., Tseng, W.-Y.I., Gau, S.S.-F., 2022. Gray matter volume alteration is associated with insistence on sameness and cognitive flexibility in autistic youth. Autism Res. https://doi.org/10.1002/aur.2732.
Silson, E.H., Steel, A., Kidder, A., Gilmore, A.W., Baker, C.I., 2019. Distinct subdivisions of human medial parietal cortex support recollection of people and places. https://doi.org/10.7554/elife.47391 eLife.
Skandalakis, G.P., Komaitis, S., Kalyvas, A., Lani, E., Kontrafouri, C., Drosos, E., Liakos, F., Piagkou, M., Placantonakis, D.G., Golfinos, J.G., Fountas, K.N., Kapsalaki, E.Z., Hadjipanayis, C.G., Stranjalis, G., Koutsarnakis, C., 2020. Dissecting the default mode network: direct structural evidence on the morphology and axonal connectivity of the fifth component of the cingulum bundle. J. Neurosurg. 134, 1334–1345.
Slocombe, C.S., 1926. The measurement of intelligence. J. Educ. Psychol. 17, 600–607.
Slocombe, C.S., 1927. Why the IQ is not, and cannot be constant. J. Educ. Psychol. 18 (6), 421–423. https://doi.org/10.1037/h0072908.
Smith, E., Thurm, A., Greenstein, D., Farmer, C., Swedo, S., Giedd, J., Raznahan, A., 2016. Cortical thickness change in autism during early childhood. Hum. Brain Mapp. 37, 2616–2629.
Turkheimer, E., Haley, A., Waldron, M., D'Onofrio, B., Gottesman, I.I., 2003. Socioeconomic status modifies heritability of IQ in young children. Psychol. Sci. 14, 623–628.
Vogt, B.A., Nimchinsky, E.A., Vogt, L.J., Hof, P.R., 1995. Human cingulate cortex: surface features, flat maps, and cytoarchitecture. J. Comp. Neurol. 359, 490–506.
Vogt, B.A., Vogt, L., Laureys, S., 2006. Cytology and functionally correlated circuits of human posterior cingulate areas. Neuroimage 29, 452–466.
Voorhies, W.I., Miller, J.A., Yao, J.K., Bunge, S.A., Weiner, K.S., 2021. Cognitive insights from tertiary sulci in prefrontal cortex. Nat. Commun. 12, 5122.
Weiner, K.S., 2019. The Mid-Fusiform Sulcus (sulcus sagittalis gyri fusiformis). Anat. Rec. 302, 1491–1503.

Weiner, K.S., Willbrand, E.H., 2023. Is there an association between tuber involvement of the fusiform face area in autism diagnosis? Ann. Neurol. https://doi.org/10.1002/ana.26632.
Weiner, K.S., Golarai, G., Caspers, J., Chuapoco, M.R., Mohlberg, H., Zilles, K., Amunts, K., Grill-Spector, K., 2014. The mid-fusiform sulcus: a landmark identifying both cytoarchitectonic and functional divisions of human ventral temporal cortex. Neuroimage 84, 453–465.
Weiner, K.S., Natu, V.S., Grill-Spector, K., 2018. On object selectivity and the anatomy of the human fusiform gyrus. Neuroimage 173, 604–609.
Welker, W., 1990. Why does cerebral cortex fissure and fold? In: Jones, E.G., Peters, A. (Eds.), Cerebral Cortex: Comparative Structure and Evolution of Cerebral Cortex, Part II. Springer US, Boston, MA, pp. 3–136.
Willbrand, E.H., Parker, B.J., Voorhies, W.I., Miller, J.A., Lyu, I., Hallock, T., Aponik-Gremillion, L., Koslov, S.R., Null, N., Bunge, S.A., Foster, B.L., Weiner, K.S., 2022a. Uncovering a tripartite landmark in posterior cingulate cortex. Sci. Adv. 8, eabn9516.
Willbrand, E.H., Voorhies, W.I., Yao, J.K., Weiner, K.S., Bunge, S.A., 2022b. Presence or absence of a prefrontal sulcus is linked to reasoning performance during child development. Brain Struct. Funct. 227, 2543–2551.
Willbrand, E.H., Bunge, S.A., Weiner, K.S., 2023a. Neuroanatomical and functional dissociations between variably present anterior lateral prefrontal sulci. J. Cognit. Neurosci. 35, 1846–1867.
Willbrand, E.H., Ferrer, E., Bunge, S.A., Weiner, K.S., 2023b. Development of human lateral prefrontal sulcal morphology and its relation to reasoning performance. J. Neurosci. https://doi.org/10.1523/JNEUROSCI.1745-22.2023.
Willbrand, E.H., Maboudian, S.A., Kelly, J.P., Parker, B.J., Foster, B.L., Weiner, K.S., 2023c. Sulcal morphology of posteromedial cortex substantially differs between humans and chimpanzees. Commun. Biol. 6, 1–14.
Willbrand, E.H., Parker, B.J., Weiner, K.S., 2023. Individual differences, missing sulci, and nomenclature: A comment on “On presentation of the human cerebral sulci from inside the cerebrum". J. Anat. 243, 1066–1068. https://doi.org/10.1111/joa.13932.
Willbrand, E.H., Tsai, Y.-H., Gagnant, T., Weiner, K.S., 2023d. Updating the Sulcal Landscape of the Human Lateral Parieto-Occipital Junction Provides Anatomical, Functional, and Cognitive Insights. https://doi.org/10.7554/elife.90451 eLife.
Woolnough, O., Rollo, P.S., Forseth, K.J., Kadipasaoglu, C.M., Ekstrom, A.D., Tandon, N., 2020. Category selectivity for face and scene recognition in human medial parietal cortex. Curr. Biol. https://doi.org/10.1016/j.cub.2020.05.018.
Wu, Y., Sun, D., Wang, Y., Wang, Y., Ou, S., 2016. Segmentation of the cingulum bundle in the human brain: a new perspective based on dsi tractography and fiber dissection study. Front. Neuroanat. 10, 84.
Yamasaki, S., Yamasue, H., Abe, O., Suga, M., Yamada, H., Inoue, H., Kuwabara, H., Kawakubo, Y., Yahata, N., Aoki, S., Kano, Y., Kato, N., Kasai, K., 2010. Reduced gray matter volume of pars opercularis is associated with impaired social communication in high-functioning autism spectrum disorders. Biol. Psychiatr. 68, 1141–1147.
Yang, D.Y.-J., Beam, D., Pelphrey, K.A., Abdullahi, S., Jou, R.J., 2016. Cortical morphological markers in children with autism: a structural magnetic resonance imaging study of thickness, area, volume, and gyrification. Mol. Autism. 7, 11.
Yao, J.K., Voorhies, W.I., Miller, J.A., Bunge, S.A., Weiner, K.S., 2022. Sulcal depth in prefrontal cortex: a novel predictor of working memory performance. Cereb. Cortex. 33, 1799–1813.
Zielinski, B.A., Prigge, M.B.D., Nielsen, J.A., Froehlich, A.L., Abildskov, T.J., Anderson, J. S., Fletcher, P.T., Zygmunt, K.M., Travers, B.G., Lange, N., Alexander, A.L., Bigler, E. D., Lainhart, J.E., 2014. Longitudinal changes in cortical thickness in autism and typical development. Brain 137, 1799–1812.
Zilles, K., Armstrong, E., Schleicher, A., Kretschmann, H.-J., 1988. The human pattern of gyrification in the cerebral cortex. Anat. Embryol. https://doi.org/10.1007/bf00304699.